

# HiSST: 4th International Conference on High-Speed Vehicle Science Technology 22 -26 September 2025, Tours, France



# Hypersonic Flight Missions and recent Technology Advances by

**Mobile Rocket Base** 

Frank Scheuerpflug<sup>1</sup>, Thomas H. Röhr<sup>2</sup>, Dorian A. Hargarten<sup>3</sup>, Markus Wittkamp<sup>4</sup>, Rainer Kirchhartz<sup>5</sup>

## **Abstract**

Founded as a launch service provider for sounding rocket flight missions in the sixties, Mobile Rocket Base (MORABA) has conducted more than five hundred sounding rocket missions. For the longest time, focus of the research supported was on astronomy, atmospheric physics and microgravity research. Beginning in the new millennium, hypersonic research and testing has become a relevant field of engagement, spurring developmental efforts to adapt our traditional sounding rocket portfolio and flight systems to the special needs of the field. This encompassed advances in thermal hardening of exposed flight structures and suppressed trajectory designs providing flight Mach numbers up to eight for more than two minutes. Four missions also involved vehicle configurations that deviated from the traditional, rotational symmetry of sounding rockets, posing new challenges to flight stability. The present paper discusses the challenges and potential of utilizing sounding rockets in hypersonic research and presents technical adaptations demonstrated by the Mobile Rocket Base. A summary is given of the to date fourteen missions in service of hypersonic research from the perspective of flight performance and technical advances. Last, we provide an outlook on current developments aiming to meet the demand for Mach numbers in excess of ten and heavier and more complex payload designs.

Keywords: Sounding Rocket, Hypersonic Flight Test

## **Nomenclature**

Latin

 $c_p$  – isobaric heat capacity

h – enthalpy

*Pr* – Prandtl number

*p* – pressure

q – heat flux density

*u* − airflow velocity

x – space coordinate

Greek

 $\mu$  – dynamic viscosity

 $\rho$  – density

Subscripts

aw – adiabatic wall

SP – stagnation point

w - wall

e – boundary layer edge condition

 $\infty$  – freestream condition

HiSST-2025-KEYNOTE-SPEECH 3 Hypersonic Flight Missions and recent Technology Advances by Mobile Rocket Base

<sup>&</sup>lt;sup>1</sup> Team Lead, Mobile Rocket Base, DLR Oberpfaffenhofen, Frank.Scheuerpflug@dlr.de

<sup>&</sup>lt;sup>2</sup> Systems Engineer, Mobile Rocket Base, DLR Oberpfaffenhofen, Thomas.Roehr@dlr.de

<sup>&</sup>lt;sup>3</sup> Systems Engineer, Mobile Rocket Base, DLR Oberpfaffenhofen, Dorian.Hargarten@dlr.de

<sup>&</sup>lt;sup>4</sup> Team Lead, Mobile Rocket Base, DLR Oberpfaffenhofen, Markus. Wittkamp@dlr.de

<sup>&</sup>lt;sup>5</sup> Head of Department, Mobile Rocket Base, DLR Oberpfaffenhofen, Rainer.Kirchhartz@dlr.de

#### 1. Introduction

## 1.1. Historic Roots and Research Domains of Sounding Rockets

Sounding rockets have played a crucial role in scientific exploration since the mid-20th century, offering a cost-effective and flexible platform for suborbital research. Initially developed for upper-atmosphere studies and early space science, these rockets have since become indispensable tools for a wide range of applications, including microgravity experiments, atmospheric measurements, and technology validation. In the 1960s, as interest in European aerospace capabilities grew, Germany established the Mobile Rocket Base (MORABA) under the auspices of the German Aerospace Center (DLR), providing infrastructure and expertise for launching sounding rockets and balloons. Since then, DLR MORABA has conducted more than five hundred flight missions, offering tailored flight opportunities for universities, space agencies, and industry. The vast majority of these missions focused on atmospheric physics and research under microgravity conditions, supporting disciplines ranging from materials science to life sciences.

# 1.2. Step into Hypersonics Testing

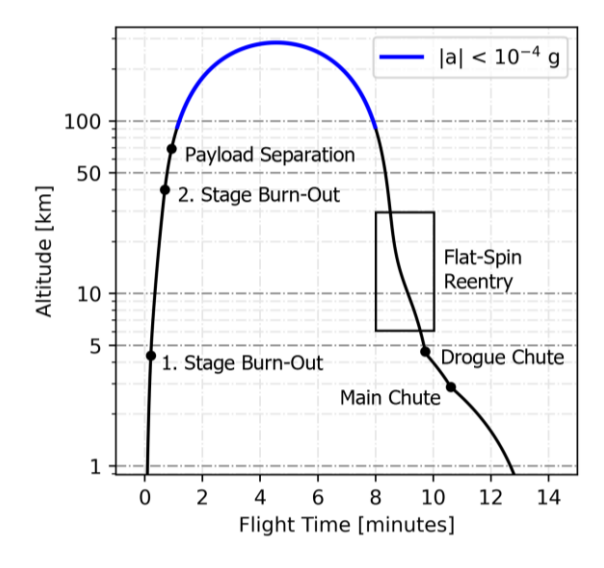
Building on its long-standing expertise in sounding rocket operations, DLR MORABA entered the field of hypersonic flight experimentation in the early 2000s to support research into re-entry and high-speed technologies. This development began with the SHEFEX (Sharp Edge Flight Experiment) program, initiated by DLR as the first dedicated hypersonic flight experiment. The program aimed to investigate innovative thermal protection systems and aerodynamic characteristics at hypersonic velocities using sounding rockets as test platforms. The success of SHEFEX demonstrated MORABA's capability to conduct high-speed flight experiments and laid the groundwork for further involvement in hypersonic research. Since then, MORABA has continued to support both international collaborations - such as those in the context of the HIFiRE-program and DLR's own technology development in the hypersonic regime, providing reliable access to short-duration, high-altitude test environments for advanced aerodynamic and re-entry studies.

# 2. Trajectory and Mission Design in Hypersonic Research

Traditional research domains mandate quick and almost vertical passage through the atmosphere to conduct the actual experiment outside or in the higher layers of the atmosphere, see Fig. 1. At altitudes typically above 65 km, the rocket motor is separated from the payload to prepare the payload for experimentation and re-entry. Upon re-entry, the payload's cylindrical shape initiates a flat spin motion, thereby quickly reducing flight speed to below 100 m/s. Eventually, two-stage parachute recovery is initiated at about four kilometers above ground.

## 2.1. Up-and-Over Trajectories

The heritage, steep parabolic trajectory design has been adopted for hypersonic research by adjusting the mission design to exploit both the up- and the downleg portion of the trajectory as an experimental window, see Fig. 2. This is most simply achieved by a captive flight of the payload, i.e. the payload remains attached to the fin stabilized rocket motor throughout the flight. A cold gas attitude control maneuver may be performed during the exo-atmospheric flight period to align the vehicle axis with reentry flight vector. This type of mission design is accordingly dubbed "Up-and-Over". Depending on the desired range of flight conditions, experimental windows typically last several seconds.



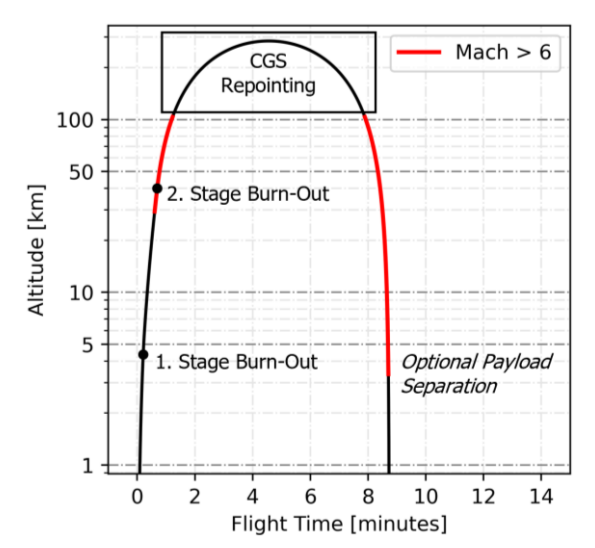


Fig. 1: Mission concept of traditional sounding rocket research involving a steep, parabolic trajectory, payload separation and parachute recovery

Fig. 2: Adjusted mission concept ("Up-and-Over") for hypersonic research involving captive flight and exo-atmospheric cold gas attitude control (CGS) to re-entry vector

# 2.2. Suppressed Trajectories

The valuable experiment duration can be significantly extended, if the trajectory design is modified to a suppressed trajectory design. Here, a vehicle comprising two or more stages is launched at a comparably shallow launch angle (typically 65°-75° range). A coast phase after first stage burnout is used to perform a gravity turn and further shallow the flight path angle before upper stages provide final impulse. Initial launch angle and coast phase duration in such a scenario present the modifiable variables of an optimization problem, which can for example aim to maximize the Mach number profile over a desired altitude band. Apart from experiment duration in the order of typically above two minutes, suppressed trajectories also offer much more steady freestream conditions compared to Up-and-Over designs.

The cost incurred with suppressed designs are however manifold and severe. While mechanical flight loads are comparable, thermal flight loads and integral heat flux typically reaches a multiple of the traditional magnitudes. Trajectory dispersion is increased, as the atmospheric density gradient amplifies any stochastic deviation from the nominal flight path. If left uncompensated, this may result in dispersion estimates that challenge the scientific objective of the mission. The large distances travelled necessitate powerful telemetry transmission equipment and reduce the number of eligible launch ranges sharply. And last, payload recovery becomes increasingly difficult when the impact location is hundreds of kilometers down range, especially when launching over the open sea.

# 3. A Comparative Analysis of Hypersonic and Heritage Trajectories

In the present chapter, we want to provide a measure of the differences and challenges associated with hypersonic trajectory designs over heritage trajectories employed in e.g. microgravity research. We carry this comparison out based on our Red Kite – Black Brant Mk4 launch vehicle (see Fig. 3), which we consider our workhorse launch vehicle for the upcoming future with its first flight planned for October 2025 within the DLR ATHEAt<sup>6</sup> flight research project [1]. Fig. 3 and Table 1 provide a schematic overview and main propulsive characteristics.

<sup>&</sup>lt;sup>6</sup> Advanced Technologies for High Energetic Atmospheric Flight of Launcher Stages



Fig. 3: Red Kite - Black Brant Launch Vehicle

Table 1: Propulsive characteristics of the Red Kite - Black Brant launch vehicle [2, 3]

Property	Red Kite	Black Brant Mk4	
Burn Time	13 s	26.5 s	
Propellant Mass	910 kg	1005 kg	
I_sp (Vac.)	2510 m/s	2535 m/s	
Max. Thrust (Vac.)	240 kN	97 kN	
First Stage Mass	ca. 1270 kg	ca. 1290 kg	

In a traditional domain mission ("**Heritage**"), e.g. a microgravity focused launch mission from Esrange, this vehicle will typically launch a heavy payload (500-600 kg) on a trajectory with an apogee of 285 km. The impact area at Esrange dictates an impact ground range of 75 km, which is achieved by a nominal launch elevation of 88.5°.

In hypersonics application, the same vehicle may carry a hypersonic payload with a mass of 300 kg on either an Up-and-Over trajectory ("**Up-and-Over**") with an apogee of 480 km or a suppressed trajectory ("**Suppressed**"), targeting an apogee of 55 km. In the latter case, optimization of the mission sequence for Mach number at apogee yields a launch elevation of 64° and a nominal coast phase between first stage burnout and second stage ignition of 30 s.

#### 3.1. Dwell time in the Hypersonic Regime

Fig. 4 presents the flight paths resulting from six degree of freedom trajectory predictions for the three trajectory designs. Fig. 5 compares the resulting dwell time in the hypersonic flight regime. The suppressed trajectory yields 3 min 24 s of hypersonic travel in the altitude band 15-55 km as compared to 34 s in the Up-and-Over variant. Notably, the duration of the experimentation period (here understood as dwell time within a certain altitude band) is a function of the trajectory apogee only, as we are limiting our considerations to ballistic flight. Significant further extension of the experimentation period becomes possible with lift-generating vehicles.

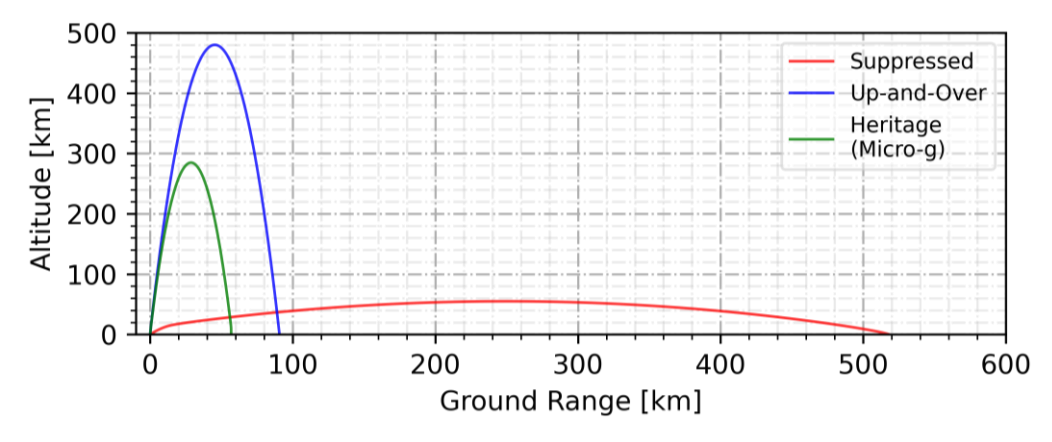


Fig. 4: Comparison of a typical Up-and-Over and a suppressed trajectory for the Red Kite — Black Brant launch vehicle

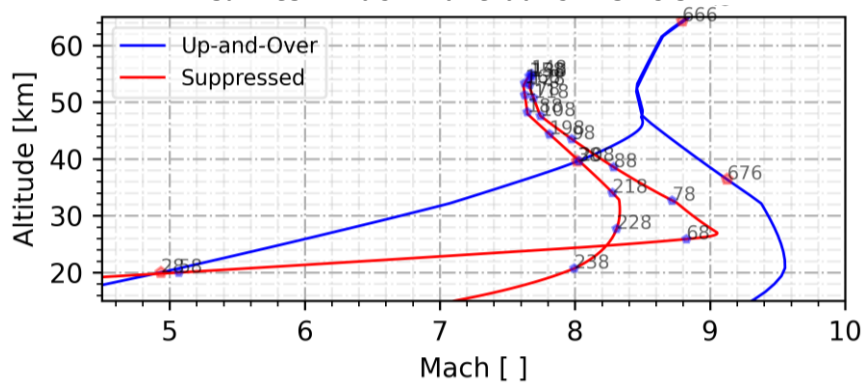


Fig. 5: Comparison of dwell time in hypersonic regime (ticks indicate flight time in 10 s intervals)

#### 3.2. Aerodynamic Heating

An accurate quantitative assessment of aerodynamic heating requires a coupled analysis of external airflow, heat transfer through the vehicle surface, and internal heat conduction. These models are inherently complex, prone to error, and demand meticulous attention from the engineer as well as substantial computational resources.

However, we can derive an estimate of the ratio of the heat loads of two different trajectories analytically. For this purpose, the stagnation point heat flux density is calculated at each mission point using the Van Driest approximation for spherical blunt bodies (Eq. 1), assuming a calorically perfect gas [4, p. 309 f.].

$$q_w = 0.763 Pr^{-0.6} (\rho_e \mu_e)^{0.5} \sqrt{\left(\frac{du_e}{dx}\right)_{SP}} (h_{aw} - h_w)$$
 (1)

Anderson [4] derives the velocity gradient at the stagnation point using Newtonian theory:

$$\left(\frac{du_e}{dx}\right)_{SP} = \frac{1}{R_N} \left(\frac{2(p_e - p_\infty)}{\rho_e}\right)^{0.5} \tag{2}$$

The subscript "e" in the equations refers to the conditions at the boundary layer edge, which at the stagnation point are derived from normal shock relations. With Pr = 0.72 for air, dynamic viscosity  $\mu_e$  modelled according to Sutherland's law [4, p. 292] and approximation of adiabatic wall enthalpy by total flow enthalpy  $h_{aw} = h_0$ , we are left to assume some spherical radius  $R_N$  and wall temperature  $T_W$  (recall that  $h_W = c_p T_W$  for calorically perfect gas). As we see from (1), the heat flux scales negatively linear with  $T_W$  and inversely proportional to  $R_N$ . However, since we aim for a comparative estimate of different trajectories only, our choice of radius and wall temperature becomes less relevant. For our

600 Stagnation Point Heat Flux Density [W/cm<sup>2</sup>] 20 30 400 10 40 200 40 30 20 100 200 300 400 500 600 700 Flight Time [s]

considerations, we use representative values of  $R_N = 1$  cm and  $T_W = 293$  K. For the trajectories given we arrive at the heat flux densities given in Fig. 6.

Fig. 6: Comparison of heat flux density (ticks indicate altitude)

**Up-and-Over** 

Heritage (Micro-g)

Suppressed

By integration over the time series, we arrive at the integral heat loads. For the Up-and-Over variant, it amounts to 19 kJ/cm², of which merely 3.2 kJ/cm² are absorbed during the ascent phase. The heat load absorbed during the ascent of the heritage mission is merely 2.3 kJ/cm², the flatspin re-entry of the payload adds another 1.5 kJ/cm². For the suppressed variant, a total of 39 kJ/cm² are absorbed. This illustrates the additional thermal protection demand raised by the usage of the downleg of the trajectory as a second experiment window and, the even higher protection demands posed by suppressed trajectories.

We should highlight one strong assumption employed in this model, which is the proposition of constant wall temperature throughout the trajectory. In reality, the flight structure skin will heat up quickly and attain high surface temperature, diminishing the heat flux to values significantly below the model. The results generated are therefore considered useful only in relation.

## 3.3. Mechanical Flight Loads

Mechanical flight loads caused by high-speed atmospheric flight may be subdivided into quasi-static and dynamic loads. Dynamic loads include aeroelastic behavior of flight structures as well as vibration and are not treated here as they are most commonly also disregarded in the preliminary design of sounding rocket launch vehicles. Firstly, this is due to a lack of models which reconcile high predictive power with ease of application. Secondly, our heritage of flight failures and anomalies harbors some which were attributed to excessive static loads, but few, if any, which could possibly be related to excessive dynamic loads.

To derive quasi-static design limit loads as the basis of flight structures design, we extract the flight conditions from the nominal trajectory of the mission. For each mission point, the aerodynamic pressure distribution over the entire vehicle is estimated, assuming a certain, fixed angle of attack. A rigid body kinetic model of the vehicle is then employed to derive loads on flight structures such as fins and interstage structures. Compliant with intuition, this model shows a proportionality of flight loads to aerodynamic loads and as those in turn scale dominantly with dynamic pressure (neglecting the dependency of aerodynamic derivatives on Mach regime), a comparison of flight loads can conveniently be reduced to a comparison of dynamic pressure.

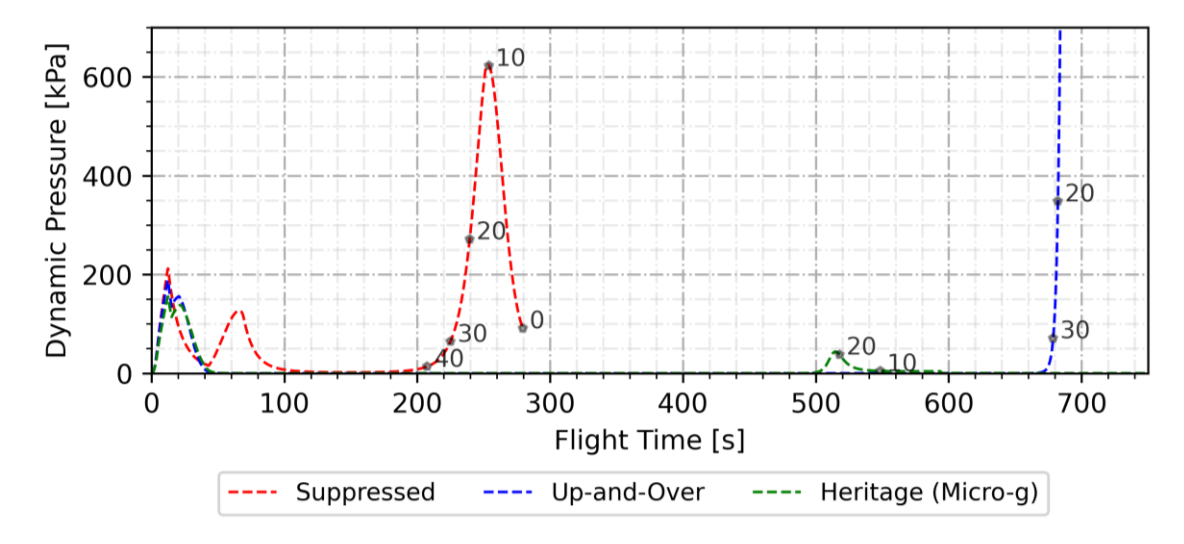


Fig. 7: Comparison of dynamic pressure (ticks indicate altitude)

Fig. 7 shows this measure for both trajectory representatives. Maybe surprisingly, the dynamic pressure during the ascent phase is of the same order of magnitude for the variants. A structural reinforcement of heritage launch vehicle components is not necessarily mandatory for applications in hypersonic mission designs, unless maybe the very late flight phase below 20 km of altitude need be survived with high probability.

## 3.4. Trajectory Dispersion

To obtain estimates of trajectory dispersion we conduct error analyses assuming a set of stochastic, normally distributed perturbation factors commonly used in the analysis of unguided sounding rocket vehicles, see [5] for details. Their combined effect on vehicle trajectories is estimated by a root-sumsquare of the effect of any single factor. Results are given in Table 2.

	Apogee Dispersion (3-sigma)	Impact Dispersion Downrange (3-sigma)	Impact Dispersion Crossrange (3-sigma)	
	[km]	[km]	[km]	
Up-and-Over	±33	±90	±72	
Suppressed	±21	±145	±46	

**Table 2: Trajectory dispersion estimates** 

Interestingly, the crossrange dispersion is much larger for the Up-and-Over ( $\pm 72$  km) than for the Suppressed variant ( $\pm 46$  km), and vice versa when it comes to downrange dispersion. This is because the crossrange dispersion basically scales with the trajectory path length which is 970 km for the Up-and-Over versus 540 km for the Suppressed variant. The relation of downrange dispersion is inverted ( $\pm 90$  km for Up-and-Over vs.  $\pm 145$  km for Suppressed), because the shallow flight path of the Suppressed variant leads to much longer dwell time inside the atmosphere which amplifies the effect of any disturbance. For instance, a drag lower than nominal (due to e.g. an overshoot in drag prediction models) will lead to increased vehicle velocity and altitude. At higher altitude however, the drag becomes even more reduced because of lower air density.

The apogee dispersion is  $\pm 21$  km for the Suppressed vs.  $\pm 33$  km for the Up-and-Over variant. Even though it may be lower by value for the Suppressed trajectory, it is more significant here, as it translates into a more severe uncertainty of the flight regimen to be expected by the experimenter. This may be unacceptable to a fraction of hypersonic test payloads requiring tightly defined flight conditions such as scramjet experiments. To address this problem, techniques to mitigate dispersion effects were developed, which we describe in chapters 4.2 and 4.3.

## 3.5. Payload Recovery

Hypersonic mission designs conflict with recovery requirements. This is because the downleg part of the trajectory is exploited as an experiment window with the vehicle travelling at hypersonic speeds, often times down to altitudes below 20 km. A conventional payload recovery in contrast would be prepared much higher up in the atmosphere by payload separation and a subsequent aerobrake manoeuvre which exploits the high drag generated by the flat-spinning payload. The payload typically decelerates to a terminal descent velocity around 100 m/s before parachute sequence is then initiated at about 4 km altitude, see Fig. 8.

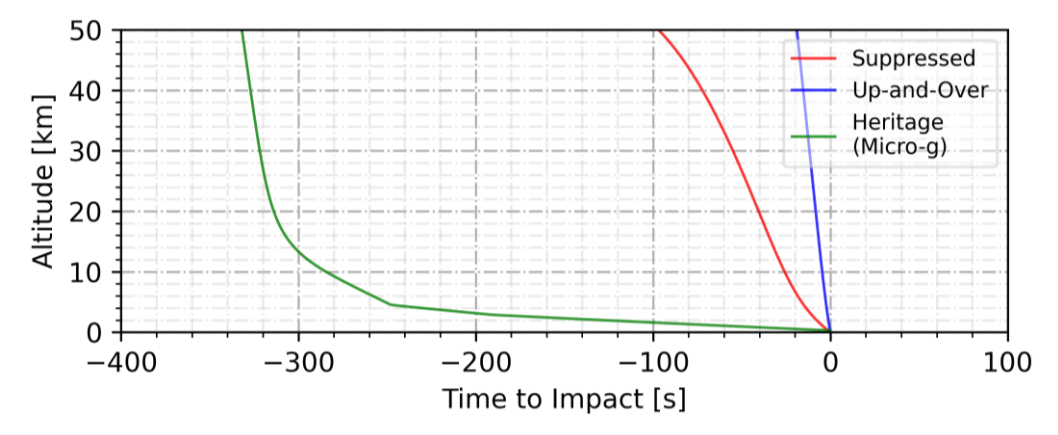


Fig. 8: Comparison of a traditional recovery sequence using a stratospheric aerobrake manoeuvre versus hypersonic trajectory designs

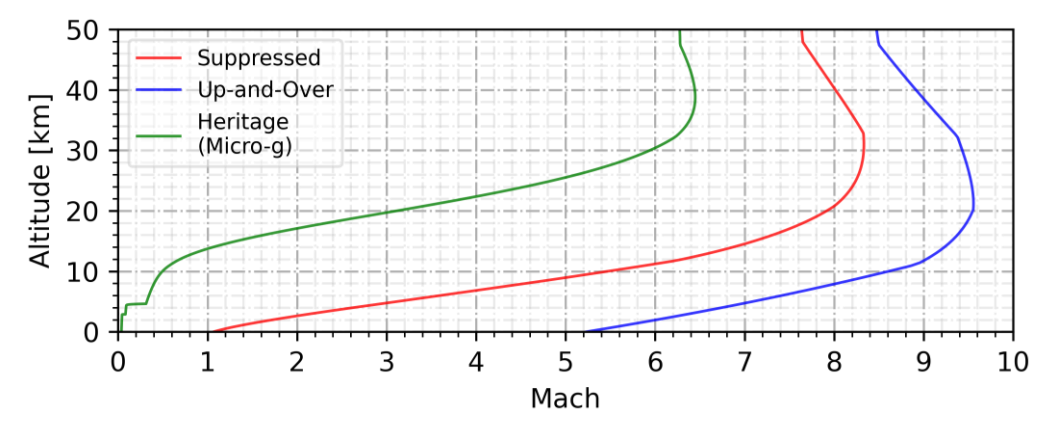


Fig. 9: Comparison of Mach numbers during late phase flight

Fig. 8 and 9 compare this archetypal heritage mission re-entry and parachute sequence to our hypersonic sample trajectories (which assuming a captive, stable flight until impact). At 15 km altitude, the payload flatspin of the heritage mission has already reduced the Mach number to 1.3. In contrast, the hypersonic variants at this point move at Mach 7.1 (Suppressed) and 9.3 (Up-and-Over). Until impact, merely 33.5 s (Suppressed) and 6.5 s (Up-and-Over) are left, which of course makes recovery challenging to realize.

In case of an impact zone over the open sea (which at current is our only viable option for impact ranges > 350 km) the requirement for a reliable sea recovery system and the demands related to the sheer distance of the impact zone from the mainland further complicate payload recovery.

# 3.6. Telemetry Coverage

As payload recovery can become demanding and risky in hypersonic mission designs, it is often times dismissed in the mission design. All data gathered during the flight must then be transmitted to the ground before the telemetry link to the vehicle is lost. Fig. 10 shows the dependency of loss of signal (approximated as line-of-sight distance and thereby conservatively neglecting beam diffraction effects) from vehicle ground range distance and flight altitude.

Fig. 10: Loss of signal (line-of-sight) from a launch site TT&C station as a function of test article altitude and ground range distance.

The graph illustrates that telemetry coverage becomes critical for ground range distances beyond 500 km assuming that coverage shall be granted down to 20 km of experimental flight. In these cases, a secondary down range station may be required to retrieve the data reliably.

# 4. Technological Advances

In this chapter, we highlight adaptions of our launch vehicles which we employed to address the challenges laid out in the previous sections, and make hypersonic research and particularly suppressed trajectories possible.

## 4.1. Thermal Hardening

For the longest time, MORABA had been coating exposed flight structures with the epoxy twocomponent based FIREX™ RX-2376. The thermal protection obtained with the compound proved marginally acceptable for heritage missions. Fig. 11 shows a fin returned from the second stage of a TEXUS<sup>7</sup> microgravity research flight – the FIREX is almost entirely consumed and the metal sheet leading edge and aluminum cover sheets show distinct buckling and blow up attributed to excessive heating. This was acceptable for a microgravity research mission, as the fin merely needed to survive the ascent, but indicated a need for stronger reinforcement as we began the design of hypersonic captive carry missions. An effort started in 2014 to find and characterize a higher performing substitute identified resin infiltrated cork as a viable option [6]. The material is widely used in space applications related to ablative thermal protection and commercially available as sheet material. As opposed to FIREX, which could be spray painted to any surface geometry, the cork-based sheet material is bonded to flight structures using epoxy adhesive. Application to surfaces demands some manufacturing attention especially when it comes to two-dimensionally curved surfaces as are found on nosecones. Appropriate techniques were developed and early flight tests showed very satisfying results [6]. Today, we apply cork based thermal protection in adjustable thicknesses to nosecones, fins, tailcans, motoradapter and motors themselves, see Figures 12-15 and 44.

Fig. 11 also shows buckling of the metal sheet leading edge used earlier. It is caused by the build-up of a strong thermal gradient during flight. The hot tip expands, but the expansion is restricted by the much cooler base, causing thermal strain and eventually buckling of the tip. The buckling could be observed in real-time during the descent of SHEFEX-1, see Fig. 26. In preparation of more demanding trajectories, we changed the design for a glass fibre reinforced phenolic resin, which proved much more capable due the superior ablative and thermal conductivity characteristics of the material, see Figures 12-15.

\_

<sup>&</sup>lt;sup>7</sup> Technologische Experimente Unter Schwerelosigkeit – the longest standing, European sounding rocket microgravity research program with more than sixty flights since 1977



Fig. 11: Heritage FIREX protected S30 fin used on a microgravity Up-and-Over trajectory (TEXUS-48, 2011) after recovery.



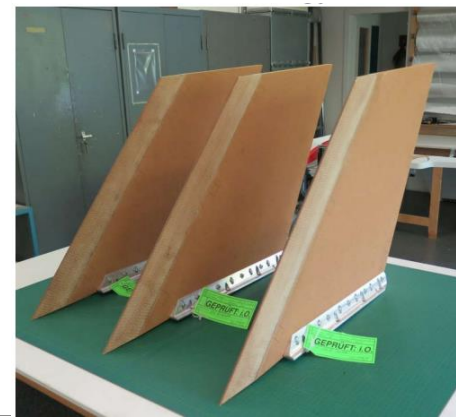


Fig. 12: Cork based thermal protection applied to nosecone and fins



Fig. 13: Fully corked tailcan assembly (MAPHEUS-78, 2018)



Fig. 14: Fin glow at second stage burnout (MAPHEUS-15, 2024)



Fig. 15: Charred second stage tailcan assembly post-flight (MAPHEUS-7, 2018)

## 4.2. Trajectory Dispersion Mitigation by Autonomous Upper Stage Ignition

The deviating effect of dispersion factors on the trajectory is very much concentrated on the first stage operation. This is because the vehicle velocity is the lowest directly after launch rail exit and perturbations from a wind gust or thrust misalignment affect the vehicle attitude much more than during later phases where dynamic pressure and aerodynamic stiffness is high. Also, errors in launcher settings obviously take effect during the launch phase.

We exploit this circumstance to achieve considerable reduction of trajectory dispersion by implementing an onboard algorithm that determines the second stage ignition instant as a function of flight state during the coast phase subsequent to first stage burn:

HiSST-2025-KEYNOTE-SPEECH 3 F. Scheuerpflug, T. Röhr, D. Hargarten, M. Wittkamp, R. Kirchhartz

<sup>&</sup>lt;sup>8</sup> MAPHEUS (Material Physics Experiments Under Weightlessness) is a DLR microgravity research program

Fig. 16: Autonomous upper stage ignition - onboard data flow

The optimizer runs a simplified trajectory prediction model on the flight computer and aims to meet the target apogee [1]. This technique eliminates the majority of apogee and downrange deviation inflicted during first stage ascent, as the direct comparison shown by Fig. 17 and Fig. 18 shows.

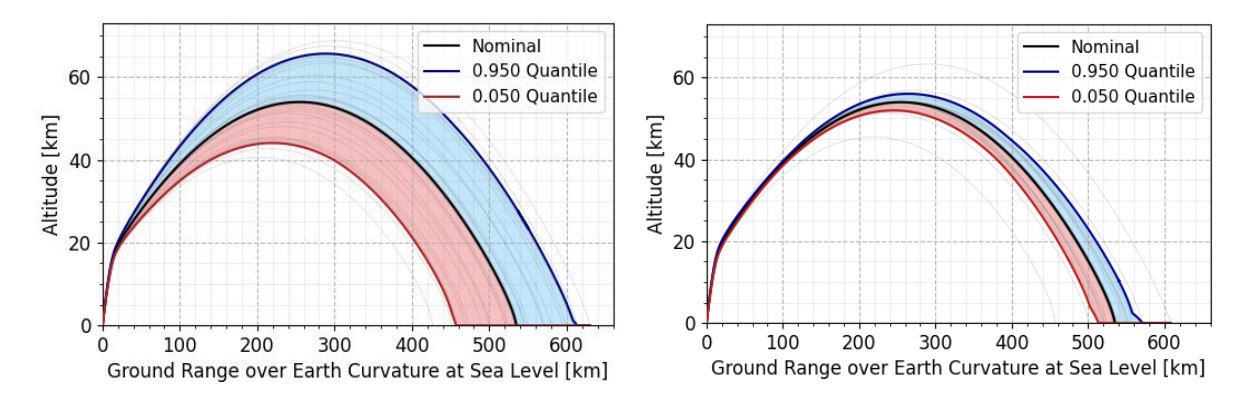


Fig. 17: Suppressed trajectory and 90% dispersion envelope with fixed second stage ignition time

Fig. 18: Suppressed trajectory and 90% dispersion envelope with autonomous second stage ignition timing

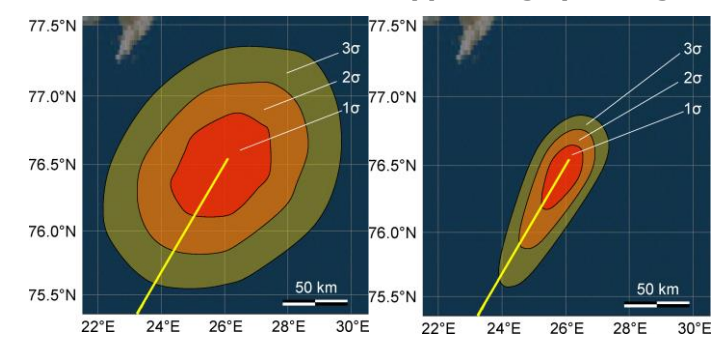
The first and to date only flight utilizing this technique was the DLR STORT mission, see chapter 5.11. Its application requires only minor adaptions in vehicle hardware. In particular, a flight termination system is not needed, as the vehicle will not change its main launch direction in case of a malfunction of the algorithm command chain. The cost to benefit ratio is therefore very high and we plan frequent application for upcoming suppressed flights.

## 4.3. Trajectory Dispersion Mitigation by Upper Stage Attitude Control

To mitigate the otherwise unacceptably large dispersion of the two-staged SHEFEX-2 (details in chapter 5.3), we leveraged our experience with cold gas attitude control of payloads to control the SHEFEX-2 upper stage attitude. The principle is to eliminate the effect of the trajectory deviation generated during the first stage burn and ascent phase by correcting the second stage attitude prior to its ignition. The algorithm used in SHEFEX-2<sup>9</sup> extracts the flight state from the Navigation System (consisting of a Global Navigation Satellite System GNSS and an inertial measurement unit IMU) and commands optimized second stage attitude angles targeting the nominal impact point, see Fig. 19. A reduction of impact dispersion of 78% is achieved, see Fig. 21. The actual flight of SHEFEX-2 covered 800 km in downrange and impacted 8 km long of the nominal impact point [7], see Fig. 21.

<sup>&</sup>lt;sup>9</sup> The algorithm was implemented in the ground segment due to technical limitations of the onboard system and human supervision on the ground. It therefore necessitated real-time up- and downlink with the vehicle.

Fig. 19: Schematic of SHEFEX-2 upper stage pointing control



20: SHEFEX-2 impact dispersion reduction (left: without correction, right: with upper stage attitude control) [5]

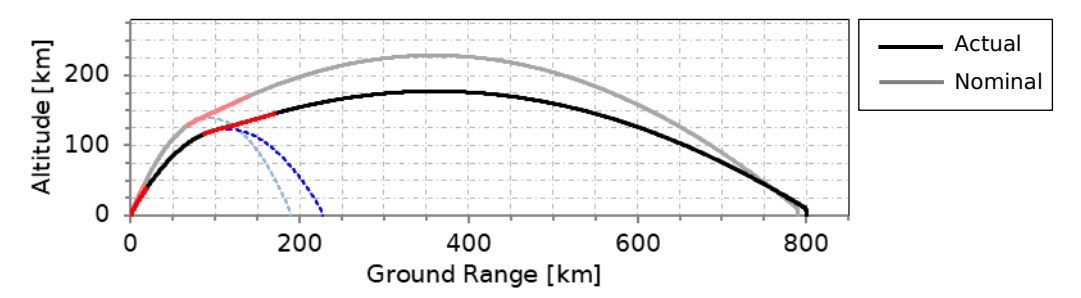


Fig. 21: SHEFEX-2 nominal and actual trajectory [7]

This technique is more powerful than a mere adaption of the upper stage ignition timing because it also allows to control crossrange dispersion. As however in case of a system malfunction, the system may effect a second stage ignition in a direction way off the nominal launch direction, implementation of a flight termination system is mandatory, which adds to vehicle complexity and cost. Also, the technique requires the vehicle to exit the atmosphere with the first stage which limits application to very powerful booster stages and disallows trajectory designs with apogees below 100 km.

# 4.4. Advances in Data Handling and Downlink Rates

The difficulties and risks associated with payload recovery as discussed in chapter 3.5 incentivize exclusion of payload recovery from mission concepts. Storing large amounts of data onboard to retrieve it post-flight is often times not an option. In consequence, our hypersonic activities are driving a desire for high rate, real time data downlink.

In 2005, the SHEFEX-1 on-board computer (OBC) was very limited in processing power. Several printed circuit boards were needed to accommodate single-core microcontrollers. It was a distributed computing system with some hardware features to speed up data output. The computers of SHEFEX-1 and -2 required two of these circuit boards. One for higher-level control tasks and distribution of uplink data and the second to generate telemetry frames with forward error correction bits for each byte sent. Each of the boards had access to a modem chip which received and decoded uplink data at a rate of 19.2 kbit/s.

Since BOLT-1 a newly developed OBC was introduced for hypersonic missions [8]. The OBC uses a large FPGA (Field Programmable Gate Array) to generate multiple telemetry streams with aggregated data rates of up to 32 MBit/s in common uses cases. The chip allows flexible telemetry setups like frequency diversity and split systems with data sent via different transmitters and mixes of both. The latter is used for the upcoming ATHEAt mission, see Table 3. In addition to the FPGA, a dual-core signal processor is used for demanding software tasks and the forwarding of IP (Internet Protocol) data. The support of IP over Ethernet is in itself a significant improvement of the onboard systems in MORABA, as it allows higher flexibility compared to the previously established RS422 serial interfaces due to its standardized protocol stack. If uplink is required, the OBC uses two improved modems of a similar type that enables a bandwidth of 38.4 kBit/s.

Many missions require live video from the onboard systems. In SHEFEX-1, two PAL (Phase Alternating Line) cameras with 625 lines were used, which were multiplexed on a single transmitter. Today's systems still support this analogue video standard and offer up to eight video sources, which are time-division multiplexed to two transmitters. More recently, we introduced IP cameras and utilize the downlink data stream for high-resolution video transmission.

Another improvement since SHEFEX-1 was the introduction of time synchronization of data streams from distributed instruments on the vehicle, allowing more precise correlation of sensory data post-flight. In SHEFEX-2, this was realized by a software-based system which synchronized with the GNSS pulse-per-second and forwards the derived signal to the instrumentation. The current OBC achieves a much higher precision of synchronization through the use of FPGA logic. It offers more flexibility through various time synchronization options with properties that can be tailored on a mission-specific basis [9].

Mission	Downlink [kBit/s]	Uplink [kBit/s]	Time-sync
SHEFEX-1 (2005)	156.25	19.2	-
SHEFEX-2 (2012)	833	19.2	software based 1 ms
BOLT 1 (2021)	1000 + 3 x 9375	Not used	FPGA based 1 ms
ATHEAt (2025)	20000	Not used	FPGA fake PPS 1 Hz constant frequency

Table 3: Characteristics of selected missions for up-, downlink and time-sync

# 4.5. Recovery in Hypersonic Missions

When the impact zone is land-based, payload recovery may be attempted very cost-efficiently by a simple separation of the motor right after completion of the experiment at about 15 km. This causes an aerodynamically unstable payload to flip almost instantly, reducing the descent velocity at high rate. We have attempted this in the ROTEX-T mission (see chapter 5.8) with success. According to GNSS data, the payload impact occurred at a velocity of around 100 m/s, see Figs. 22 and 23. Data storages inside the payload had been designed shock proof and survived the impact.

For launches of hypersonic missions over the open sea, we have to date only once attempted a parachute recovery in the SHEFEX-1 mission. The attempt failed due to a correctable error (see chapter 5.1 for details). Albeit challenging, costly and risky, we see no principal problem with the recovery of a hypersonic payload from the sea and expect to realize this in the years to come.







Fig. 22: Digging for the payload of ROTEX-T

Fig. 23: ROTEX-T payload components after recovery [10]

# 5. A Summary of Hypersonic Missions Accomplished

In this chapter, we provide a comprehensive review of published missions launched by MORABA and dedicated to a hypersonic research objective. Table 4 gives a summary of these missions. The subsections to follow provide details on each single mission including flight results and learnings from the perspective of the launch vehicle design.

Table 4: A summary of flight missions with hypersonic research objective launched by MORABA

Mission & Launch Date & Launch Range	Research Objective	Payload Gross Mass [kg]	Trajectory Type	Apogee [km]	Max. Mach
SHEFEX-1 10/2005 Andøya	Re-entry technology	200	Up-and-Over	211	6.4
HIFiRE-5 04/2012 Andøya	Aerothermo- dynamic fundamentals	undisclosed	Up-and-Over	50 (planned 300) [11]	3.1 (planned 7) [11] 2 <sup>nd</sup> stage ignition failure
SHEFEX-2 06/2012 Andøya	Re-entry technology	710	Semi-suppressed with 2 <sup>nd</sup> stage attitude adjustment	177	9.3
HIFiRE-3 09/2012 Andøya	Scramjet	undisclosed	Up-and-Over	345 [12]	8 [13]
Scramspace 09/2013 Andøya	Scramjet	150 [14]	Up-and-Over	undisclosed (planned 340) [15]	2 (planned 8) [16] 1 <sup>st</sup> stage failure
03/2015 HIFiRE-7 Andøya	Scramjet	undisclosed	Up-and-Over	undisclosed	undisclosed (planned 7.8) [13]

HIFiRE-5B 05/2016 Woomera	Aerodynamic fundamentals	undisclosed	Up-and-Over	278 [17]	8 [18]
07/2016 ROTEX-T Esrange	Aerothermo- dynamic fundamentals	190	Up-and-Over	183	5.1
HIFiRE-4 07/2017 Woomera	Glider	undisclosed	Semi-suppressed	undisclosed (planned 292) [19]	undisclosed (planned 8) [19]
BOLT 06/2021 Esrange	Aerothermo- dynamic fundamentals	163 [20]	Up-and-Over	78 (264 planned) [21]	3 (7 planned) [21] 2 <sup>nd</sup> stage pitch- roll coupling
STORT 06/2022 Andøya	Aerothermo- dynamic fundamentals	200	Suppressed with online 3 <sup>rd</sup> stage ignition control	38	8
HIFLIER 10/2023 Esrange	Aerothermo- dynamic fundamentals	395 [22]	Up-and-Over	190 [23]	6.2 [23]
SOAR 11/2023 Andøya	Ramjet Inlet	310	Up-and-Over	71	4.6
BOLT-1B 09/2024 Andøya	Aerothermody namic fundamentals	undisclosed	Up-and-Over	254 [24]	7 [24]

#### 5.1. SHEFEX-1

The DLR Sharp Edge Flight Experiment (SHEFEX) was our first launch mission dedicated to hypersonic research. The project aimed to investigate the concept of a thermal protection system comprised of flat ceramic tiles, promising elevated aerodynamic efficiency and cost-effective manufacturing [25]. The test flight was to provide real flight data that would be used to verify and calibrate numerical modelling. The mission design featured an Up-an-Over trajectory and an exo-atmospheric cold gas manoeuvre to align vehicle axis with re-entry vector. The forebody shown in Fig. 24, was asymmetrically shaped to provide data for both convex and concave surface shapes. At the time, we had no experience or models suited to assess the effect of the lifting forebody on the flight stability of the unguided S30-Improved Orion launch vehicle (Fig. 25). Leveraging on best practice of our heritage in traditional research domains, we covered the forebody under an ogival nosecone which was separated after the ascent. This of course limited the generation of scientific data to the downleg part of the trajectory.







Fig. 25: SHEFEX-1 on the U3 launcher



Fig. 26: leading edge buckling during re-entry at an altitude of approximately 25 km

An apogee of 211 km was achieved and scientific data was generated down to 14 km altitude [25]. The flight attempted to recover the payload by means of a parachute recovery system, and at this point nominally initiated the payload separation to decelerate. Unfortunately, the subsequent parachute sequence was inadvertently initiated almost immediately after the payload separation due to an unexpected pressure spike in the baro-switch trigger. The vehicle was still hypersonic and the drogue chute was destroyed due to excessive loads.

For the first time, we had an outboard camera mounted to the second stage and could observe smoke from the ablation of FIREX on the fins as well as the leading edges glowing and finally buckling from the heat and thermal stress, see Fig. 26. This experience spurred the development of phenolic leading edges and replacement of FIREX with the much more capable cork, see chapter 4.1.

## 5.2. **HIFIRE-5**

From 2009 to 2018, MORABA was a cooperation partner to Defence, Science and Technology Group (DSTG) in the Hypersonic International Flight Research Experimentation (HIFiRE) program which was jointly conducted by DSTG, the US Air Force Research Laboratory, BAE Systems and the University of Queensland. The main goal of this program was to gather basic research data on aspects of hypersonic flight that are not easily obtainable in ground-based wind tunnels [13]. MORABA was selected to conduct five flight missions within the program.

The mission numbering was oriented along the technological objectives, and HIFiRE-5 was the first flight to be conducted by MORABA. The purpose of the mission was to investigate the hypersonic flow and boundary layer transition [13] around an elliptical forebody, see Fig. 28. An S30-Improved Orion was selected as launch vehicle, see Fig. 27. An Up-and-Over trajectory design was employed with target apogee of 300 km. The flight was planned as a captive carry down to impact and carried out in April 2012. The second stage failed to ignite, which could later be attributed to a hangfire event in the ignition chain. This resulted in a reduced apogee of only 50 km (vs. 300 km targeted) and maximum Mach number of 3.1 instead of the planned 7 [11].





Fig. 27: HIFiRE-5 on the Athena Launcher (image used with permission from DSTG)

Fig. 28: Perspective onto the elliptically shaped forebody (image used with permission from DSTG)

#### 5.3. SHEFEX-2

SHEFEX-2 (Sharp Edge Flight Experiment) was a two-stage sounding rocket mission to investigate advanced re-entry technology. The launch was conducted from Andøya Space in June 2012. Comprising a suppressed trajectory, initiated by a cold-gas pointing maneuver prior to second stage ignition, and spanning 800 km over the Norwegian sea [7], it was the most complex sounding rocket mission ever carried out by the German Aerospace Center DLR. Its scientific objective was to expand the data basis of real flight data of sharp-edged re-entry bodies [26]. Beyond the achievements of SHEFEX-1, the mission featured a more complex payload involving active cooling technologies and a canard system for the investigation of maneuver efficiency during hypersonic flight [27]. The 710 kg heavy payload should be propelled to Mach numbers up to ten on a suppressed trajectory. To meet these criteria, we adopted the two stage VS-40 launch vehicle developed by our partners at the Brazilian Insitute of Aeronautics and Space (IAE). The first stage was launched at a nominal elevation of 82.5° to ensure that the impulse delivered by the first stage (comprised of four tons of composite propellant) would safely lift the aerodynamically instable second stage out of the atmosphere. There, the second stage attitude was controlled by a cold gas system prior to second stage ignition to correct for any trajectory deviation incurred during the ascent, as described in chapter 4.3. The correction algorithm was tailored to meet the nominal impact location 800 km down range. Indeed, the actual first stage trajectory deviated 2.5 σ from nominal, but the correction of the second stage ignition vector ensured an impact as close as 8 km to nominal [7].



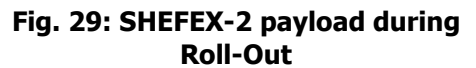




Fig. 30: SHEFEX-2 on the U3 launcher

### 5.4. HIFIRE-3

The objective of HIFiRE-3 was to test an axisymmetric, hydrogen fueled supersonic combustion experiment in real flight condition [13]. As in HIFiRE-5, an S30-Improved Orion was selected as launch vehicle. The flight had initially been scheduled for a double campaign with HIFiRE-5, but was deferred to September of 2012 to allow for investigation and resolve of the second stage ignition failure that occurred on the HIFiRE-5 flight.



Fig. 31: HIFiRE-3 on the Athena launcher (image used with permission from DSTG)

# 5.5. Scramspace

Scramspace was a scramjet research mission mandated by the University of Queensland. The mission concept was based on the S30-Improved Orion utilizing an Up-and-Over trajectory and exo-atmospheric separation of the scramjet experiment, which was designed as a free flyer [16]. To obtain aerodynamic stability, the payload featured large fins, which degraded the overall stability of the launch vehicle. Strakes were added between the four second stage fins as compensation. Exo-atmospheric cold gas attitude control to align with re-entry vector was also accomplished by the free flying payload [16]. The flight suffered a failure of the first stage nozzle which generated sufficient lateral thrust and impairment of the fin assembly structure by the hot gas jet to destabilize the vehicle during first stage burn. A joint failure investigation involving our partners Defence Science and Technology Group (Australia) and Institute of Aeronautics and Space (Brazil) established an improved manufacturing process and elevated structural margin of the failed nozzle assembly.



Fig. 32: Artists impression of the Scramspace payload mid-flight (image used with permission from Sandy Tirtey)



Fig. 33: Strakes between the fins of the second stage for improved aerodynamic stability

#### 5.6. HIFIRE-7

HIFiRE-7 was a free-flying, hydrogen fueled scramjet experiment which aimed to produce real-flight data of two symmetrically arranged Rectangular-to-Elliptical Shape Transition (REST) scramjets, [31]. The symmetric payload (see Fig. 34) was covered by an ogival nosecone during the ascent phase to ensure dynamic stability of the launch vehicle and protect the scramjet. Payload separation was initated after the atmospheric ascent, after which the payload pursued self-dependent exo-atmospheric cold gas re-orientation and re-entry and experiment phase. A VSB-30 was selected as launch vehicle for its increased performance compared to the S30 - Improved Orion (approx. 200 kg more payload on similar trajectory [28]) which had been used in HIFIRE-5 and HIFIRE-3. The VSB-30 had been developed between 2001 to 2004 by the Brazilian Insitute of Aeronautics and Space IAE in cooperation with MORABA [29] and at that time had accomplished fourteen of our microgravity research missions at 100% success rate [30]. With the payload being relatively short and protruding outside the motor diameter slightly (hammer-head), the launch vehicle was modified to a 4/4 fin configuration to provide sufficient static stability, see Fig. 35. The launch was carried out in March of 2015 from Andøya Space. The launch vehicle provided a close to nominal insertion of the payload and also separation and reorientation worked well. The mission was therefore acknowledged as successful, even though the failure of an onboard telemetry component due to excessive heating upon re-entry caused loss of a significant amount of scientific data [31].





Fig. 34: The HIFiRE-7 free-flyer scramjet payload during rollout (image used with permission from DSTG)

Fig. 35: HIFiRE-7 on the U3 launcher (image used with permission from DSTG)

## 5.7. HIFIRE-5B

As the flight experiment conducted with HIFiRE-5 failed to provide the desired hypersonic transition data, a re-flight of the experiment was successfully launched in May 2016, this time from Woomera Test Range [18], see Fig. 37. Launch vehicle and payload were essentially identical to the precursor flight [18].



Fig. 36: HIFiRE-5b second stage during integration (image used with permission from DSTG)



Fig. 37: HIFiRE-5b on the Woomera Launcher (image used with permission from DSTG)

#### **5.8. ROTEX-T**

DLR's research mission ROTEX-T (Rocket Technology Experiment – Transition), launched in July 2016 from Esrange, focused on boundary layer condition over a biconical payload, see Fig. 38. Cost was dominantly driving the mission design. For this reason, a surplus Terrier Mk12 – Improved Orion was selected as launch vehicle. Also, inertial navigation and exo-atmospheric attitude control were excluded from the design. Instead, re-alignment of the vehicle was left to passive stabilization and amplitude damping by the densifying atmospheric conditions upon re-entry. Sensory data was recorded at rates far beyond telemetry capacity and therefore stored onboard in impact-hardened solid-state storage devices. Upon reaching 13 km on the downleg, the payload was separated from the motor and decelerated to below 100 m/s until the intended hard impact (see also Fig. 22). The payload was successfully recovered and the data retrieved [10].



Fig. 38: ROTEX-T payload during environmental testing



Fig. 39: ROTEX-T on the medium range launcher

### 5.9. HIFIRE-4

The scientific purpose of HIFiRE-4 was to gather flight data on the aerodynamics, stability, and control of an advanced waverider at speeds approaching Mach 8. The mission launched successfully in July 2017 from the Woomera Test Range in South Australia on a semi-suppressed trajectory with planned apogee 292 km [19]. Launch vehicle used was a VSB-30 in 4-4 fin configuration. First time, we employed the thermally improved second stage fin design described in chapter 4.1. The payload consisted of two configurationally identical gliders [19], which were mounted belly to belly atop the second stage and covered by an ogival nosecone during the ascent phase. Upon reaching space, the gliders were released, each equipped with nitrogen gas thrusters for orientation and aerodynamic control surfaces (elevons) for in-atmosphere maneuvering after re-entering the atmosphere.



Fig. 40: HIFiRE-4 on the Athena (image used with permission from DSTG)

#### 5.10. BOLT

Boundary Layer Transition (BOLT) aimed to deepen the understanding of laminar-turbulent boundary layer transition in the hypersonic regime. Significant progress in this field had been achieved by HIFiRE, particularly flight 5B. Building on this success, a new experiment was devised by the US Air Force Research Laboratory (AFRL) and Air Force Office of Scientific Research (AFOSR) that would replace the elliptical forebody of HIFiRE-5b with a more complex shape featuring concave surfaces and highly swept leading edges as shown in Fig. 41. The experiment was designed and built by the principle investigator, the Applied Physics Laboratory (APL) of Johns Hopkins University [32]. BOLT was launched in June 2021 on a two-stage S31-Improved Orion vehicle [20]. Due to dynamic instability during the second stage burn phase, large angles of attack caused loss of kinetic energy. This resulted in reduced apogee of only 78 km (vs. 264 km planned) and reduced flight Mach number of merely 3 (vs. 7 planned). Payload recovery had been attempted by a baro-initiated payload separation, but failed as the vehicle reached ground before the flight sequencer armed the separation circuit. Stable impact occurred at Mach 1.3, burying the payload beyond reach (Fig. 43). Postflight analysis later identified pitch-roll coupling due to different aerodynamic coefficients of the non-axisymmetric forebody in pitch and yaw combined with aeroelastic static margin reduction as the most likely cause [21]. BOLT spurred two successful follow-up flights, Boundary Layer Turbulence (BOLT-2) launched at NASA Wallops in 2022 [33], as well as BOLT-1B described later.



Fig. 41: BOLT Payload during Environmental Testing (image reproduced with permission from Johns Hopkins Applied Physics Laboratory)



Fig. 42: BOLT on the MAN2 launcher



Fig. 43: BOLT impact hole

## **5.11. STORT**

The DLR experiment STORT (Schlüsseltechnologien für hochenergetische Rückkehrflüge von Trägerstufen) aimed to investigate the behavior of high-temperature ceramic materials, active cooling and health monitoring technologies in a long duration, high enthalpy air flow [34]. The experiment mandated direct insertion of its 200 kg payload into the stratosphere at Mach 8 on a suppressed trajectory. This performance lay beyond the capacity of the two-stage workhorse VSB-30, triggering the development of the three stage S31-S30-Improved Orion vehicle. The mission concept foresaw a launch at a nominal 68° elevation and passive separation of the S31 booster after burnout at T+11.5 s. After a coast phase of 12.5 s to leverage gravity turn, the second stage burn was initiated, which propelled the vehicle to Mach 4.7 during its 27 s burn time [35]. The second stage was separated by an active separation mechanism. A second gravity turn maneuver followed to align the flight trajectory with the mission requirement. The instant of third stage ignition was determined by the flight computer in real time to meet the target apogee with precision. The flight reached an apogee of 38 km, providing Mach numbers around eight for a duration of 70 s. Fig. 44 shows the vehicle on the launcher. The S31

booster had been modified to carry six fins to provide sufficient stability during early flight. As the first stage flight speed barely reached Mach 1, the S31 was not equipped with any thermal protection. The second stage only received protection on fins and the conical third stage adapter. The third stage was fully covered in cork- and zirconium-dioxide-based protection.



Fig. 44: STORT on the U3 Launcher

#### 5.12. SOAR

The Red Kite is a solid propellant rocket motor developed with the application as a powerful booster for multi-staged sounding rockets in mind [2]. With SOAR (Single Stage Operational Assessment of Red Kite), a single stage test flight was conducted in November 2023 with the primary mission objective being the flight qualification of the new motor [36]. The flight also carried a rotationally symmetric ramjet inlet as passenger payload [37]. The large amount of air flowing through rather than around the payload sparked concerns with regards to flight stability, particularly under off-design conditions and unintended transients such as an unstart condition of the inlet. The vehicle was equipped with additional static margin by a fourth fin and the ramjet inlet was kept closed by means of a movable central cone during the booster burn phase to ensure no impairment of the primary mission objective. The mission used an Up-and-Over trajectory and reached an apogee of 71 km. Re-alignment of the vehicle with flight vector on the downleg was left to passive aerodynamic stabilization.



Fig. 45: SOAR before Roll-Out

# 5.13. HIFLIER

The Hypersonic Integrated Flight Research and Experimentation (HIFLIER) combined an AFRL experiment measuring second-mode boundary layer instability and transition on a cone with 7 ° half-angle [38] with a DLR experiment demonstrating in-flight transpiration cooling of porous C/C-SiC composite fins [23]. The two experiments were stacked on a single-stage Black Brant vehicle as shown in Fig. 46. HIFLIER was launched in October 2023 at Esrange reaching Mach 6.2 and an apogee of 190 km on an Up-and-Over trajectory. Unfortunately, although the payload could be tracked by GNSS until late in the flight, the helicopter recovery crew was not able to spot the payload around the predicted impact location in the Swedish tundra; it has to date not been found. Nonetheless, valuable data was received via telemetry including according to AFRL 'the first conclusive proof of the presence of second-mode instability waves in hypersonic flight' [39].

Notably, HIFLIER was the first mission since the 1990s in which DLR utilized the Black Brant solid rocket motor. We consider this motor, manufactured by Magellan Aerospace [3], uniquely suited for hypersonic research. Its long and slender shape keeps drag low and brings high static stability even for light-weight payloads. We expect it to be used for many more hypersonic research missions in the coming years.



Fig. 46: HIFLIER lift-off from the MAN2 launcher

#### 5.14. BOLT 1B

Scientifically a re-flight of the failed BOLT mission, BOLT-1B was successfully launched in September 2024 from Andøya Space. While the experiment forebody was very similar, a single-stage Black Brant V was selected as launch vehicle for its superior characteristics with regards to dynamic stability. Based on the learnings from BOLT, extensive 6-DOF flight dynamics analyses were conducted by APL and DLR including non-axisymmetric and aeroelastic modeling of the vehicle [40]. One result of these analyses was that a zero-roll-rate scheme could help reduce angle-of-attack growth, so the fin cant angle was set to  $0.0\,^{\circ}$  instead of the usual  $0.3\,-0.4\,^{\circ}$ .

BOLT-1B reached Mach 7.1 both on the up-leg and on the down-leg, the apogee reached was 254 km. Exo-atmospheric re-pointing and re-entry angle-of-attack suppression by CGS worked well, so both science windows could be fully utilized. With a terminal roll rate of 0.45 Hz, angle-of-attack below  $1-\sigma$  (dispersion estimation) during the science windows and continuous telemetry data reception down to 6 km altitude, much valuable data could be gathered that is still being evaluated [24].



Fig. 47: BOLT-1B prepared for Roll-Out (image used with permission from Johns Hopkins Applied Physics Laboratory)

## **6. Development Trends**

More recent inquiries and preliminary discussions around hypersonic test missions divide into two directions. The first seeks to investigate basic aerothermodynamics at Mach numbers well beyond ten, sketching payloads of 200-400 kg mass. We aim to meet this demand by bringing the three staged Red Kite – Red Kite – Black Brant Mk4 into service with a first flight not before 2027. The other development direction seeks to flight test subscale or demonstrator level hypersonic free-flyers. This branch seems to target Mach numbers below or well below ten, but payloads are generally heavy and often times lifting bodies with wingspans well beyond the main diameter of the launch vehicles we currently operate. To meet this demand, we seek to employ large solid rocket motors (ranging from two to twelve ton net explosive mass) and thrust vector guidance to help insertion accuracy.

## 7. Summary and Conclusion

Since the first dedicated hypersonic experiment SHEFEX in 2005, MORABA has carried out fourteen missions in support of hypersonic flight research, eleven of which can be regarded as fully successful from a launch service provider's perspective. These missions demonstrated the feasibility of using sounding rockets for short-duration, high-speed flight experiments and provided valuable data for reentry physics, aerothermal analysis, and scramjet investigations.

Over the years, numerous adaptations were introduced to enable these demanding missions: improved thermal protection, advanced trajectory concepts such as suppressed designs, dispersion mitigation techniques, and modernized on-board computing and telemetry. As a result, MORABA can now support missions that would have been infeasible only a decade ago.

Looking ahead, the trend is twofold: on the one hand, towards deeper hypersonic regimes beyond Mach 10 using advanced multi-stage vehicles; on the other, towards heavier, more complex payloads such as free-flyers with lifting surfaces. Both paths highlight the growing role of sounding rockets as an indispensable platform for bridging the gap between ground-based testing and future operational hypersonic flight systems.

## 8. Acknowledgements

The work described was made possible and supported by experimenters and partners at Defence Science and Technology Group of Australia, University of Queensland, the US Air Force Research Laboratory, the US Air Force Office of Scientific Research and Johns Hopkins University. Particularly, we would like to express gratitude for the continuous support and joyful collaboration with our esteemed colleagues from DLR BT-RSI, DLR AS-HYP and DLR AS-RFZ. The authors would also like to acknowledge the vision and determination delivered by the former department head of Mobile Rocket Base, Peter Turner.

#### References

- 1. Gülhan, A., Klingenberg, F., Willems, S., Hargarten, D., Ettl, J., Reimer, T., Baier, L.: Long Duration Hypersonic Flight Experiment ATHEAt, Proceedings of the 75th International Astronautical Congress (2024)
- 2. Scheuerpflug, F., Röhr, T. H., Huber, T., Hargarten, D. A., Kirchhartz, R., Kuhn, M., Weigand, A., Berndl, M., Werneth, J.: Red Kite Sounding Rocket Motor Qualification and Application Spectrum. Journal of Spacecraft and Rockets (2025), 0:0, pp. 1-13. doi:10.2514/1.A36203
- 3. Magellan Aerospace: Black Brant 5 Rocket Motor Web Version. Magellan Aerospace. https://magellan.aero/wp-content/uploads/Black%20Brant%205%20Rocket%20Motor%20-Web%20Version.pdf, Accessed 12 August 2025
- 4. Anderson, J. D., Hypersonic and high temperature gas dynamics Second Edition. AIAA (1989)
- 5. Scheuerpflug, F., Kallenbach, A., Cremaschi, F.: Sounding Rocket Dispersion Reduction by Second Stage Pointing Control. Journal of Spacecraft and Rockets, 49:6 pp. 1159-1162 (2012). doi:10.2514/1.A32193
- 6. Drescher, O., Hörschgen-Eggers, M., Pinaud, G., Podeur, M.: Cork Based Thermal Protection System for Sounding Rocket Applications Development and Flight Testing. 23rd ESA PAC Symposium (2017)
- 7. Scheuerpflug, F., Kallenbach, A.: The Flight Control of SHEFEX-2. Proceedings of the 21st ESA Symposium on European Rocket and Balloon Programmes and Related Research, SP-721, p. 357-360 (2013)
- 8. Wittkamp, M., Zigiotto, A.: A very High Performance Multi Purpose Computing Card for TM/TC and Control Systems. European Test and Telemetry Conference (2009)
- 9. Wittkamp, M., Ettl, J., Synchronous Sampling for distributed Experiments, ESA PAC Symposium 22nd Proceedings (2015)
- 10. Thiele, T., Gülhan, A., Olivier, H., Instrumentation and Aerothermal Postflight Analysis of the Rocket Technology Flight Experiment ROTEX-T, Journal of Spacecraft and Rockets 55:5, pp. 1050-1073 (2018)
- 11. Juliano, T.J., Adamczak, D., Kimmel, R.L.: HIFiRE-5 Flight Test Results, Journal of Spacecraft and Rockets 52:3, 650-663 (2015), doi:10.2514/1.A33084
- 12. Wade, M., VS-30/Orion. Encyclopedia Astronautica. http://www.astronautix.com/v/vs-30orion.html. Accessed 05.08.2025.
- Bowcutt, K. G., Paull, A., Dolvin, D. J., Smart, M.: HIFIRE: An international collaboration to advance the science and technology of hypersonic flight. 28th Congress of the International Council of the Aeronautical Sciences (ICAS), Brisbane, Australia. https://www.icas.org/media/pdf/ICAS%20Congress%20General%20Lectures/2012/ HIFIRE.pdf (2012). Accessed 01 August 2025
- 14. Clark, S.: Autopsy of a space disaster: Failure, but not a flop, Phys.org (2013). https://phys.org/news/2013-12-autopsy-space-disaster-failure-success.html. Accessed 01 August 2025
- 15. Wikipedia: Scramspace (2023). https://en.wikipedia.org/wiki/Scramspace. Accessed 25 August 2025
- 16. Tirtey, S., Boyce, R., Creagh, M., van Staden, P., Dimitrijevic, I., Capra, B.: The SCRAMSPACE I scramjet flight design and construction. 18th AIAA/3AF International Space Planes and Hypersonic Systems and Technologies Conference (2012). doi:10.2514/6.2012-5843
- 17. Defence Science and Technology Group und U.S. Air Force Research Laboratory: Hypersonic Flight Success, DST Group (2016), https://www.dst.defence.gov.au/news/2016/05/18/hypersonic-flight-success. Accessed 05 August 2025

- Kimmel, R. L., Adamczak, D. W., Hartley, D., Alesi, H., Frost, M. A., Pietsch, R., Shannon, J., Silvester, T.: Hypersonic International Flight Research Experimentation-5b Flight Overview. Journal of Spacecraft and Rockets 2018 55:6, pp. 1303-1314
- 19. Smith, T., Bowcutt, K., Selmon, J., Miranda, L., Northrop, B., Lau, K., Silvester, T., Mairs, R., Unger, E., Paull, A., Paull, R., Dolvin, D., Alesi, H.: HIFiRE 4: A low-Cost Aerodynamics, Stability, and Control Hypersonic Flight Experiment, 17th AIAA International Space Planes and Hypersonic Systems and Technologies Conference (2011), doi:10.2514/6.2011-2275
- 20. Hörschgen-Eggers, M., Kirchhartz, R.M., Jung, W., Schoppmann, K., Ettl, J., Wittkamp, M.: Boundary Layer Transit Flight Experiment: Mission Overview, Launch Vehicle and Payload Subsystems. Journal of Spacecraft and Rockets, Vol. 58, No. 1, 26–37 (2021)
- 21. Kutty, P., Butler, C., Wheaton, B.M., Fortier, J.: 6DOF Simulation Analysis for the Post-Flight Investigation of the Boundary Layer Transition (BOLT) Experiment. AIAA Aviation Forum (2022). doi:10.2514/6.2023-3672
- 22. Swedish Space Corporation: Successful launch of the HIFLIER rocket. https://sscspace.com/successful-launch-hiflier/ (2023). Accessed 14 August 2025
- 23. Di Martino, G. D., Peichl, J., Hufgard, F., Duernhofer, C., Loehle, S., Göser, J.: Main flight data on transpiration cooled sharp edge fins in hypersonic conditions on the sounding rocket HIFLIER. Aerospace Science and Technology, Vol. 158, Art. No. 109895 (2025)
- 24. McKiernan, G., Butler, C., Wolf, T., Kathrotiya, P., Kutty, P., Melcher, J. T., Wheaton, B. M., Adamczak, D. W.: Initial Results of the BOLT-1B Flight Experiment. AIAA SCITECH Forum (2025). doi:10.2514/6.2025-1339
- 25. Turner, J., Hörschgen-Eggers, M., Jung, W., Stamminger, A., Turner, P.: SHEFEX Hypersonic Re-entry Flight Experiment Vehicle and Subsystem Design, Flight Performance and Prospects. Proceedings AIAA 14th Spaceplane Systems and Technologies Conference (2006)
- 26. Weihs, H., Turner, J., Longo, J. M.: Key Experiments within the SHEFEX-2 Mission. IAC 2008, Glasgow, Scottland (2008)
- 27. Turner, J., Hörschgen, M., Ettl, J., Jung, W., Turner, P.: SHEFEX-2 Development Status of the Vehicle and Sub-Systems for a Hypersonic Re-Entry Flight Experiment. ESA SP-671, 19th ESA Symposium on European Rocket and Balloon Programmes and Related Research (2009)
- MORABA Mobile Rocket Base: MORABA Launch Vehicles [PDF]. German Aerospace Center (2020). https://moraba.de/wp-content/uploads/2020/11/MORABA\_Launch\_Vehicles\_2020-05.pdf, Accessed 01 August 2025
- 29. Palmerio, A., Silva, J., Turner, P., Jung, W.: The development of the VSB-30 sounding rocket vehicle. 16th ESA Symposium on European Rocket and Balloon Programmes and Related Research, (2003).
- 30. MORABA Mobile Rocket Base: Missions calendar Mobile Rocket Base MORABA DLR Space Operations and Astronaut Training (2025). https://moraba.de/en/current-moraba-missions/missions-calender/, Accessed 11 August 2025
- 31. Razzaqi, S. A., Silvester, T., Smart, M. K., Ross, P.: The HIFiRE 7 Flight Experiment, 22nd AIAA International Space Planes and Hypersonics Systems and Technologies Conference (2018), doi:10.2514/6.2018-5256
- 32. Wheaton, B. M.: The Boundary Layer Transition (BOLT) Flight Experiment. Johns Hopkins APL Tech. Digest, Vol. 36, No. 2, 213–223 (2022)
- 33. Portoni, P. P., Dufrene, A., Maclean, M., Wadhams, T., Kostak-Teplicek, H., Bowersox, R.D.W.: BOLT II Vehicle Design, Instrumentation, and Ground Test Comparisons to Flight. Journal of Spacecraft and Rockets, Vol. 62, No. 4, 1278–1293 (2025)
- 34. Reimer, T., Di Martino, G., Petkov, I., Dauth, L., Baier, L., Gülhan, A., Klingenberg, F., Hargarten, D. A.: Design, Manufacturing and Assembly of the STORT Hypersonic Flight

- Experiment Thermal Protection System. 25th AIAA International Space Planes and Hypersonic Systems and Technologies Conference (2023), doi: 10.2514/6.2023-3089
- 35. Gülhan, A., Hargarten, D. A., Zurkaulen, M., Klingenberg, F., Siebe, F., Willems, S., Di Martino, G., Reimer, T.: Selected results of the hypersonic flight experiment STORT. Acta Astronautica, 211, pp. 333-343 (2023). doi: 10.1016/j.actaastro.2023.06.034
- 36. Röhr, T., Scheuerpflug, F., Ettl, J., Kail, D., Mildenberger, C., Riehmer, J., Schnepf, C., Kirchhartz, R.: Flight Qualification of the Red Kite Solid Rocket Motor. 3rd International Conference on High-Speed Vehicle Science Technology (2024)
- 37. Riehmer, J., Klingenberg, F., Röhr, T., Schnepf, C., Zuber, C., Gülhan, A.: Design and Objectives of the Air-breathing Propulsion Experiment Technology Demonstrator (APEX-TD). 3rd International Conference on High-Speed Vehicle Science Technology (2024)
- 38. Borg, M.P., Adamczak, D.W., Culler, A.J., Kurtz, M.D.: HIFLIER Hypersonic Flight Experiment: Design, Analysis, and Ground Test. AIAA SCITECH Forum (2025). doi:10.2514/6.2025-0733
- 39. Borg, M.P., Adamczak, D.W., Tufts, M.W.: HIFLIER Hypersonic Flight Experiment: Ascent Results. AIAA SCITECH Forum (2025). doi:10.2514/6.2025-0734
- 40. Kutty, P., Butler, C., Melcher, J. T., Wheaton, B. M.: Flight Dynamics Modeling of the Boundary Layer Transition 1B (BOLT-1B) Experiment. Applied Aerodynamics, Vol. 2, 1309–1320 (2023)